II International Conference on Particle-based Methods - Fundamentals and Applications
PARTICLES 2011
E. Oñate and D.R.J. Owen (Eds)

COLLAPSE OF WET GRANULAR COLUMNS: EXPERIMENTS AND DISCRETE ELEMENT SIMULATIONS

FABIO GABRIELI*, RICCARDO ARTONI†, ANDREA SANTOMASO† AND SIMONETTA COLA*

* Dept. of Hydraulic, Maritime, Environmental and Geotechnical Engineering (IMAGE)
University of Padova
via Ognissanti 39, 35129 Padova, Italy
e-mail: fabio.gabrieli@unipd.it; Web page: http://www.image.unipd.it

†Department of Chemical Engineering Principles and Practice (DIPIC)
University of Padova
Via Marzolo 9, 35131 Padova, Italy
Web page: http://www.dipic.unipd.it

Key words: wet granular materials, DEM, capillary force, slope collapse, PIV

Abstract. This work aims at investigating the effect of triggering and jamming due to the addition of a small quantity of fluid to the material. Collapse of dry and wet granular columns is studied both from the experimental and the numerical point of view. Wet samples of glass beads of different grain-sizes in the pendular state were packed in a rectangular box and then allowed to flow by removing a lateral wall. The dependence of the kinematics and the final state of the system on grain size and water content was particularly investigated. DEM numerical simulations were carried out in a 1:1 scale. A good qualitative agreement between experiments and DEM simulations was found with respect to the kinematic and the final slope profile. In particular, both the techniques highlight the strong effect of the liquid which decreases the run-out distance and time even for small liquid contents. This work demonstrates the suitability of the DEM approach also for the study of wet granular materials in static as well as in dynamic conditions, however it highlights that the water redistribution model is critical for the model outcome.

1 INTRODUCTION

The triggering and jamming mechanisms are of growing interesting in many fields of science: from the statistical mechanics to the geotechnical engineering, to the material science, and to chemical processes. At a micro-scale these phenomena have been studied for the link with the formation of amorphous material like glassy systems or emulsions; at a meso-scale the interested is focused on the formation and run-out of granular flow (like landslides or controlled flows) or, in the industrial field, to the transportation an jamming of powders and grains in the process networks.

In the field of granular flows, recent research has been carried out on the collapse of granular columns, an unsteady reference problem which involves both triggering and jamming of the flow. The typical experiment is very simple: an axisymmetric or rectangular column [1, 2] is allowed to collapse by lifting respectively the containing cylinder or a containing wall. The material collapses generally evolving to a pile with a typical inclination slightly lower than the angle of repose. The position of the avalanche following triggering of the motion was usually registered in time to reconstruct the kinematics of the collapse, and the final runout distance and heap height were estimated in order to develop scaling laws for the final deposit. In the various works available in the literature, the effect of the initial aspect ratio, the size and shape of the grains, the roughness of the bottom surface was evaluated for the case of dry granular materials. For this case, discrete element simulations were also performed with different approaches (classical molecular dynamics or contact dynamics methods) generally confirming the experimental results [3, 4].Various models have also been proposed to explain the obtained experimental data [5].

In this work research on granular column collapse is extended to the study of wet granular materials, both from the experimental and the numerical point of view. Wet granular materials are very interesting because, generally, the presence of water in the granular medium greatly affects phenomena even in very small amounts [6]. This research represents a first step in the investigation of the effect of small quantity of fluid on triggering and jamming.

In this paper the dependence of the kinematics and the final state of the system on grain size and water content was particularly investigated both experimentally and numerically (through DEM). This work demonstrates the suitability of the DEM approach also for the study of wet granular materials in static as well as in dynamic conditions, however it highlights that the water redistribution model is probably critical for the model outcome.

2 MICROMECHANICS OF WET GRANULAR MATERIALS

The degree of saturation of wet granular materials can be divided into 5 states [7]: (1) completely dry when water content is zero, (2) pendular state when the air domain is connected and a little amount of water is shared by couples of grains forming the so called capillary bridge or pendular ring or meniscus, (3) funicular state when pendular rings collapse on one another and the water is shared by 3 or more solid grains, (4) capillary state when the liquid domain is connected and air is confined in some bubbles and (5) completely wet or saturated when the air content is zero. In this work it was chosen to focus on the pendular regime, which is usually considered to take place in the range w = 0-5%, where w is the weight ratio between liquid and granular material. When two particles share a little amount of fluid an attractive force exists between them. This force is due to two component namely cohesion and adhesion. The first term is related to the liquid surface tension; the second instead depends also on the properties of the solid-liquid contact. If the particles are equal and spherical and the liquid surface is symmetrical (this is reasonably true for low Bond number and low normalized capillary volume) these force mainly acts along the direction joining two particle centers and can be very high in comparison to contact forces normally experienced at the contacts.

Following Rothenburg & Bathurst [8] and Santamarina [9], normal contact forces for a random packing of dry spheres with void ratio e and coordination number m can be estimated as:

$$F_{cont,n} = 4R^2\sigma_{iso}\frac{\pi(1+e)}{m}; \tag{1}$$

One can observe that normal contact forces mainly depend on R^2 and on the depth of the particle, which mainly controls the isotropic tension σ_{iso}. On the other hand volumetrical forces (i.e. gravitational forces, unbalanced forces) depend on R^3 while maximum capillary forces are linearly proportional with R [10, 11], as it will discussed in the follow:

$$F_{cap,max} = F_{cap}\left(s=0\right) = -2\pi R\gamma\cos\phi \tag{2}$$

Viscous forces instead strongly depend on the relative velocity between particles [12], but they can be considered really small in the study of transition phase problems (static to flowing and vice versa). In figure 1 these forces are plotted as a function of particle radius depicting which force prevails from a micromechanical point of view. This graph does not take into account fluctuations of these forces that can be very important, especially for contact forces.

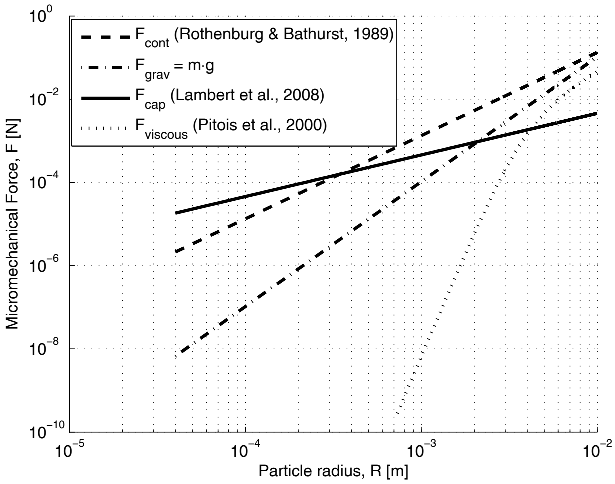

Figure 1: Typical values of different types of micromechanical forces varying particle size.

It should be noted that this graph extents down to very low particle size (typically < $4\mu m$). For lower particle radii, van der Waals interaction forces are expected to prevail, but

were not taken into account in this study. Exploring the grain size of many medium-coarse granular materials (namely sandy-silty soil in geotechnics) some interesting observation can be simply obtained. Indeed, all micromechanical forces decrease with particle size but in a different manner. Contact forces prevail for larger particle size while capillary forces in this range are very low; on the other hand for lower radius capillary forces increase and overcome contact forces. Substituting some trial values of R in equation 2 and comparing the results with the weigth of the particles with the same size, one can estimate the number of particles that can be assembled to form a vertical capillary chain. From this simple observation it should be stated that the maximum depth of influence of a particle with $R = 1$ mm at the surface of a wet granular material extends at maximum to approximately $\sim$ 8R equal to 8 mm depth. For lower particle size $R = 0.1$ mm this zone extends to $\sim$ 870R = 8.7 cm. It is clear that, in this range of grain sizes, the dynamics of wet granular materials will strongly depend on the grain size itself and on size of granulated cluster of particles.
The first solution to the problem of the capillary force existing between two spheres was developed by Haines [13] and Fisher [11] solving Young-Laplace equation for a simplified geometrical configuration: the fluid surface was approximated as a toroidal ring (see Figure 2a). Recently some authors, in order to increase the accuracy of this solution and at the same time to keep its simplicity, have provided other empirical equations based on the fitting of numerical solutions of the Young-Laplace equation for different radii, capillary volumes and gaps between particles [14, 15]. These equations represent the capillary force as a function of particle gap, contact angle and capillary volume. They obtained satisfactory results in comparison with experimental tests and allowed to extend the suitability of these equation for uneven particle size [16]. Another possible way is the use of an approximation of the so-called *minimum energy approach* that finally leads the following rational equation:

$$F_{cap}(s,V) = -\frac{2\pi R\gamma\cos\phi}{1+[s/2d(s,V)]}, \tag{3}$$

$$d(s,V) = (s/2)\left[-1+\sqrt{1+2V/(\pi R s^2)}\right], \tag{4}$$

where s is the gap, V is the capillary volume, ϕ the contact angle, γ the liquid surface tension. In addition Lian et al. [17] experimentally observed that the bridge broke when:

$$s = s_d = \left(1+\frac{\phi}{2}\right)V^{1/3}, \tag{5}$$

It can be noted that F_{cap} has a maximum value when two particles are in contact ($s = 0$) and, in this condition, it does not depend on capillary volume. F_{cap} decreases with the gap s and the larger the volume, the higher the capillary force and the maximum allowed distance between the two particles (see Figure 2b). On the other hand, in order to form a capillary bridge a gap $s < s_d$ is not sufficient, but it is necessary that the distance between particles is lower than:

$$s_c = \frac{12V}{\pi\left(1 + \frac{1}{1-\cos\phi}\right)} \tag{6}$$

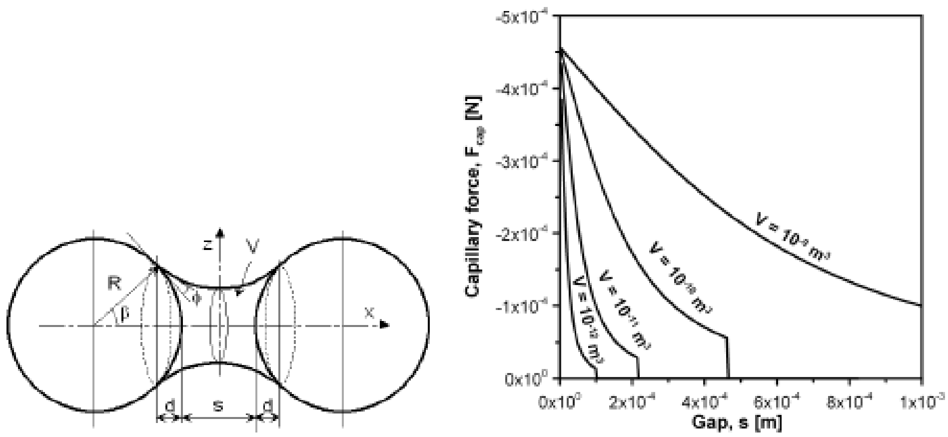

(a) (b)

Figure 2: (a) Geometry of the capillary bridge; (b) capillary force for different capillary volumes

3 MATERIALS AND METHODS

3.1 Experiments

Experiments of granular column collapse were performed in a rectangular channel as displayed in Figure 3. The channel was made of transparent glass plates, lateral walls being 35 cm long, 12 cm high, with a gap of 5 cm between them. A 5 x 15 cm glass plate was used as the removable confining wall for the experiment. As the focus of the present work was to understand the effect of wetting on collapse dynamics, and mainly to investigate different water amounts and particle diameters, the influence of the initial aspect ratio of the column (which was studied, for the dry case, in a number of experimental and numerical works) was not addressed. The initial dimension of the column was therefore kept fixed to length W_0=7 cm and height H_0=8 cm (approximately) for all the experiments and simulations. The sample was first prepared separately by mixing a certain amount of liquid to the material, which was then poured in the experimental box. The effective amount of liquid in the material was quantified by weighing the dry, empty preparing container and the container after having poured the spheres into the column. It was important to quantify precisely the amount of water in the sample since the water involved was a very scarce quantity ($\sim$ 5 mL). The experiment was performed by lifting by hand the moving wall, allowing the column to collapse freely under the action of gravity. By looking at the recorded movies, it was verified that manual lifting was sufficiently

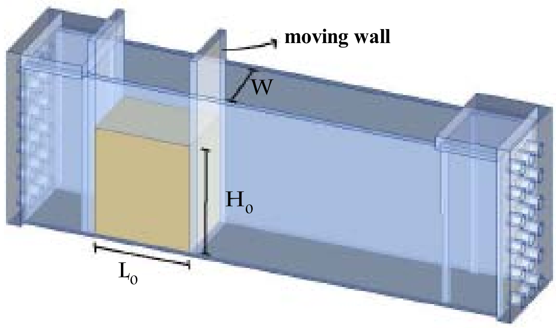

Figure 3: Sketch of the experimental channel used for the granular column collapse experiments.

reproducible.
Glass spheres in two particle sizes ($d_p = 2, 5$ mm) were used for the experiments. Given the density of glass ($\rho_p = 2532\ kg/m^3$) and the weight of the dry sample, it was possible to estimate the number of particles in the experiments, which were nearly 41000 for 2 mm and 2600 for 5 mm spheres. Two different liquid were tested: distilled water (surface tension, $\gamma = 72.75$ mN/m, contact angle $\phi = 15^o$) and water with a tensioactive ($\gamma = 17.10$ mN/m, $\phi = 40^o$), which had the effect of lowering the surface tension of water. Contact angle measurements of the two fluids on the particles were performed by taking microscopical photos of little drops on a flat glass surface. In particular, the amounts of water tested were $w = 0$ (dry), 0.5, 1., 2., 4. %. During each experiment, the evolution of the system was tracked by taking pictures at certain time intervals using a CCD camera. In particular, two cameras were used: (1) a high-speed CCD camera (Photron FastCam PCI) capable of frame rates up to 1000 fps (which was operated at 250 fps), and (2) a high resolution CCD camera (CASIO EX-F1) which was operated at 30 fps. The first camera was employed to reconstuct the instantaneous velocity field through Particle Image Velocimetry. The second camera was employed when high resolution images were required, for example for a more accurate slope evaluation.
In order to reconstruct the instantaneous velocity field from sequences of images, Particle Image Velocimetry (PIV) analysis was employed. PIV was performed using the open source MATLAB toolobox MatPIV [18], adopting an interrogation window shifting technique [19] in three steps (24x24; 24x24; 12x12) and filtering the velocity field to remove wild vectors.

3.2 Numerical simulations

From the pioneering work of Cundall and Strack [20] Discrete Element Methods (DEM) were extensively used in many field of sciences. The goodness of this method was proved with respect to many quasi-static problems [21, 22] as for steady granular flows [23]. In the original form, contact is represented by a linear spring with a dashpot in the normal direction and a linear spring, a dashpot and a frictional slider in the tangential one. The capillary force can be easily added in final form of unbalanced forces computation:

$$m\ddot{x}_i = \sum F_{cont} + \sum F_{cap} + F_{grav} \tag{7}$$

Where F_{cont} are the contact forces derived from the spring-dashpot analogical model and F_{cap} are obtained with equation 3. Another important issue regards the distribution of liquid volume. Following the evidence obtained from X-ray tomography experiments, in numerical simulations the liquid volume was equally distributed on 95% of potential contact, intending potential contact as a couple of particle that could potentially share that specific amount of volume.

The redistribution algorithm was structured as follows: when a couple of spheres sharing a meniscus detaches (when the gap s overcomes s_d) the liquid volume equally distributes on the two spheres. When a particle rotates the attached drop of liquid follows its movement, and a capillary bridge re-creates when these conditions are contemporary met: (1) the gap between the particles is lower than the formation distance s_c given in Eq. 6, and (2) the position of the drop is within a certain threshold angle from the line connecting the two spheres. For two drops to collapse to one bridge, both drops have to satisfy the requirements, otherwise at least one drop will not form a bridge.

A sample with the same geometry and dimensions, and the same number of particles of the experiments was generated and was initially prepared as a loose random packing which was then sedimented due to gravity. As the material was the same, the same contact parameters were used for sphere-sphere and sphere-wall contacts. The parameters were previously calibrated on the base of some triaxial tests at different confining stresses (normal and tangential stiffness: $k_n = 400$ kN/m, $k_s = 100$ kN/m; contact friction coefficient: $\tan\phi_\mu = 0.62$). The numerical experiment aimed at accurately reproducing the experimental set-up: the lifting movement of the moving wall was imposed, as estimated from the image sequences, to be an accelerated motion with an acceleration $a = 16\ m/s^2$.

4 RESULTS

4.1 PIV analysis

For the experiments where image sequences were collected at 250 frames per second, it was possible to perform a particle image velocimetry (PIV) analysis to reconstruct the instantaneous velocity field. Results from PIV are reported as an example in Figure 4 for the case of dry, 5 mm particles. A complete set of PIV tests was not performed due to technical reasons, and it was preferred to concentrate the efforts more on slope profiles than on instantaneous velocity fields. The dry, 5 mm test which is analysed in the Figure is however very useful to understand some important features of the phenomenon. Future efforts will concentrate on a systematic PIV campaign.

As it can be noticed in Figure 4, where the evolution of the collapse event is shown at 4 different times, after removing the confining wall the collapse starts in the lowest part of the column, setting into motion only a part of the original sample. Indeed a zone can be

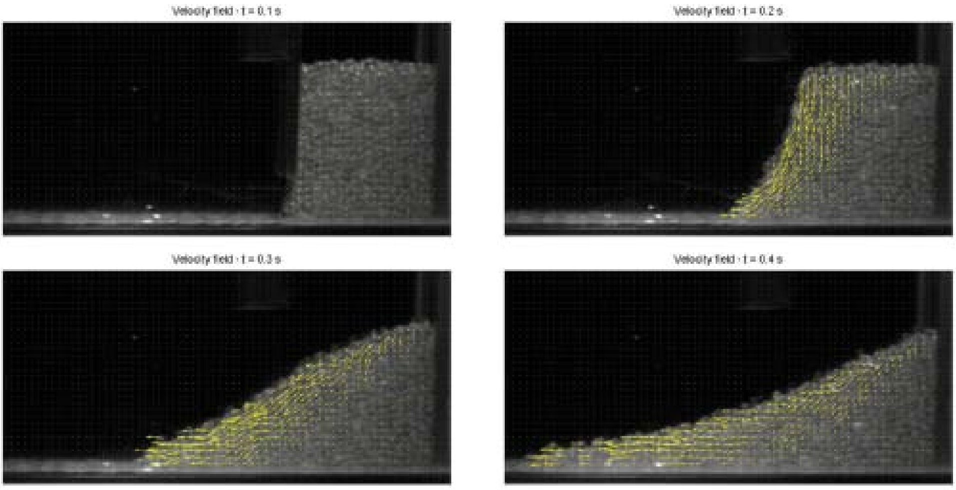

Figure 4: Results from PIV analysis of dry particles ($d_p = 5$ mm).

recognized where no motion occurs, which can be identified as a triangular zone close to the rear confining wall, containing nearly half of the material. Following Rankine theory, for cohesionless frictional material with friction angle ϕ, the soil mass interested to this movement is a triangular wedge contained between vertical and an angle of $45 - \phi/2$ with respect to vertical. The collapsing material rapidly deposits forming a slope with a uniform angle.

4.2 Kinematics

The kinematics of the collapse can be appreciated by looking at Figures 5 and 6. In Figure 5, the shape of the surface during the collapsing event is tracked for the experimental data, for dry and $w = 1\%$ samples. It is clear from the figure that the shape of the sample depends only slightly on grain size, but depends strongly on the presence of water. In particular, the figure shows that according to experience, smaller particles are more affected by the presence of water: while 5 mm particles behave, wet or dry, nearly in the same way, 2 mm particles flow in a more rigid manner and with a certain delay in comparison with completely dry particles. Then the final slope has a steeper angle and the runout length is less than in the dry case.

In figure 6, the time evolution of the normalized runout distance and the normalized maximum height of the pile is described for both experiments and simulations. Experiments show the typical sigmoid profile, composed of an accelerating zone, a zone with approximately constant velocity, and a decelerating zone. The delay in the motion of the 2 mm particles is even more clear from this figure.

As reported in the literature on dry column collapse, for the dry case the particle diameter plays no role on the dynamics. Here it is demonstrated that a small water amount is sufficient to make the particle diameter play an important role, even for coarse particles (as the 2 mm particles are).

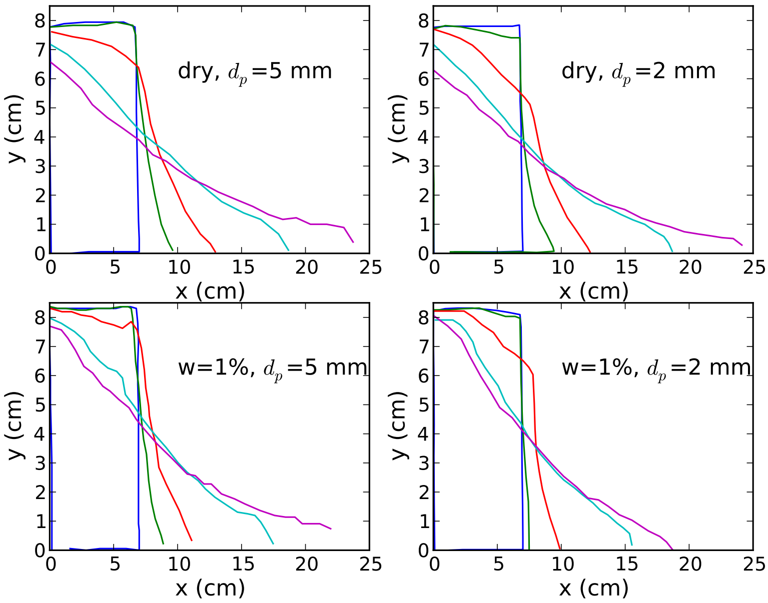

Figure 5: Slope evolution in time for some experimental tests, extrapolated from the images at times $t = \{0\ s, 0.17\ s, 0.23\ s, 0.36\ s, 0.49\ s\}$

4.3 Final deposit

The strong effect of water on the behavior of the column is clear also looking at the final values of heap height and runout length shown in Figure 7. Results show how the water content plays a strong role, particularly on 2 mm spheres, and that increasing the water content the pile gets higher and shorter. The final height of the heap is nearly the same as the initial height for wet 2 mm spheres: this suggests that the swedge-shaped static zone is more extended in the wet case. Collapse experiments performed with a different wetting fluid (with a low surface tension), for 2 mm particles, were expected to display a lower cohesive behavior; results showed that little difference exists between the two wetting fluids. On this point more accurate measurements should be performed.

4.4 Comparison between experiments and DEM calculations

It was difficult to precisely define the end of the pile particularly at the end of the simulations because of a layer of particles rolling away near the head of the front. This phenomenon is not present in the experiments probably because of the redistribution mechanism or lower restitution of the particles. For this reason it is more reasonable to compare the kinematics in the accelerating and constant velocity regions. Regarding the

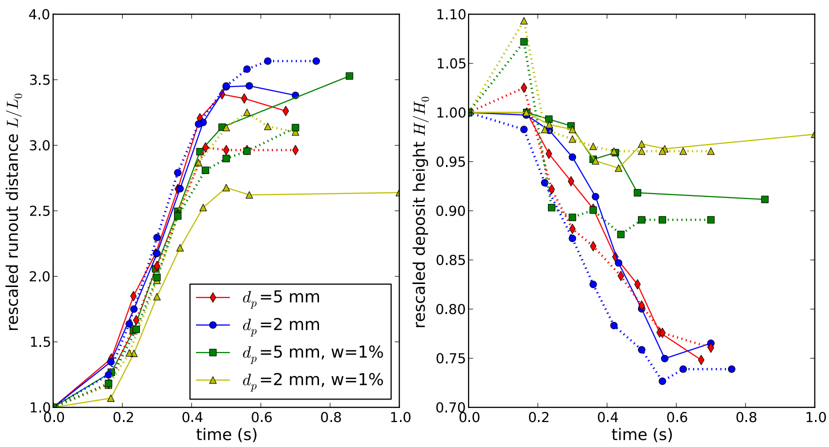

Figure 6: Comparison between experimental (solid lines) and numerical (dotted lines) results obtained for different particle diameters and for dry/wet situations: (left) length of the heap rescaled on initial length vs time and (right) height of the heap rescaled on initial height vs time.

dry results, a good qualitative agreement is found. DEM predicts a similar behavior for 2 mm and 5 mm particles in the dry case. For the wet case, the heap height variation in time is reasonably reproduced in DEM simulations, and the initial delay of wet material is also observable from the results. However, the great difference in the runout length variation in time between 2 mm and 5 mm wet particles and, in general between wet and dry samples, is not evident. It can be hypothesized that this should be due to the redistribution mechanism, which is probably not efficient enough. By looking on the final profiles and their dependence on water content, at first the dfficulty of estimating the runout length appears particularly on the case of 5 mm spheres. By looking at the figures representing variation of deposit height and final angle, it can be said that at least qualitatively the DEM approach captures the increasing of the heap angle with water content, and quantitatively predicts the final angle and height for the dry case. Once again DEM simulations seem to underestimate the effect of water, particularly on 2 mm spheres.

5 CONCLUSIONS

In this work experiments and numerical simulations have been presented for the collapse of dry and wet granular columns for different particle diameters. Experiments highlighted the strong effect of the addition of water on the kinematics and on the final slope profiles. DEM simulations, which employ a particular redistribution mechanism, appear to agree qualitatively with the experimental results. In order to reach a quantitative agreement, some refinements are needed probably on the redistribution mechanism and on particle restitution coefficients.

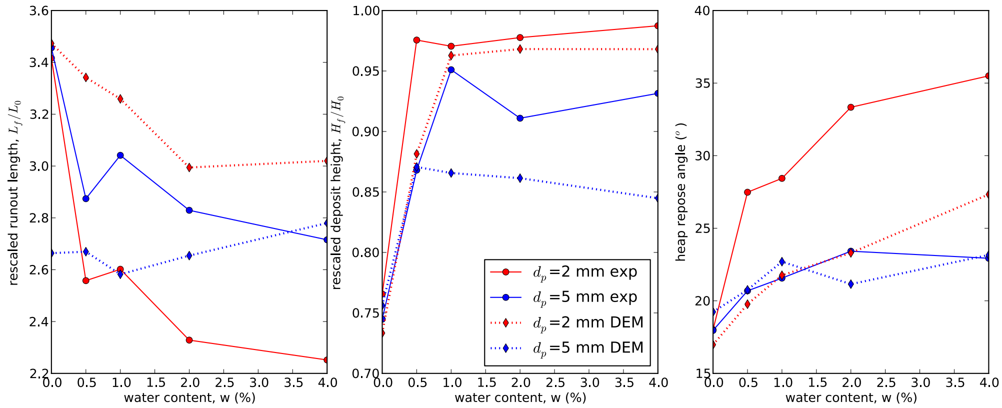

Figure 7: Experimental and numerical results obtained for different particle diameters and for different water contents: (a) Final length of the heap rescaled on initial length vs water content (b) final height of the heap rescaled on initial height vs water content (c) final heap angle versus water content.

REFERENCES

[1] Lube, G., Huppert, H., Sparks, R. and Freundt, A. Collapses of two-dimensional granular columns. *Phys. Rev. E* (2005). **72**(4):1–10.

[2] Lajeunesse, E., Monnier, J. and Homsy, G. Granular slumping on a horizontal surface. *Phys. Fluids* (2005). **17**(10).

[3] Zenit, R. Computer simulations of the collapse of a granular column. *Phys. Fluids* (2005). **17**(3):031703–1–031703–4.

[4] Staron, L. and Hinch, E. Study of the collapse of granular columns using two-dimensional discrete-grain simulation. *J. Fluid Mech.* (2005). **545**(-1):1–27.

[5] Doyle, E., Huppert, H., Lube, G., Mader, H. and Sparks, R. Static and flowing regions in granular collapses down channels: Insights from a sedimenting shallow water model. *Phys. Fluids* (2007). **19**(10).

[6] Hornbaker, D.J., Albert, R., Albert, I., Barabasi, A.L. and Schiffer, P. What keeps sandcastles standing? *Nature* (1997). **387**:765.

[7] Newitt, D.M. and Conway-Jones, J.M. A contribution to the theory and practice of granulation. *Trans. Inst. Chem. Eng.* (1958). **36**:422–442.

[8] Rothenburg, L. and Bathurst, R.J. Analytical study of induced anisotropy in idealized granular material. *Géotechnique* (1989). **49**:601–614.

[9] Santamarina, J. *Soils and waves.* John Wiley & Sons Ltd, Chichester, England (2001).

[10] Lambert, P., Chau, A., Delchambre, A. and Regnier, S. Comparison between two capillary forces models. *Langmuir* (2008). **24**(7):3157–3163.

[11] Fisher, R.A. On the capillary forces in an ideal soil; correction of formulae given by w.b. haines. *J. Agricult. Sci.* (1926). **16**:492–505.

[12] Pitois, O., Moucheront, P. and Chateau, X. Liquid bridge between two moving spheres: An experimental study of viscosity effects. *J. Colloid Interface Sci.* (2000). **231**(1):26–31.

[13] Haines, W. Studies of the physical properties of soils. ii. a note on the cohesion developed by capillarity forces in an ideal soil. *J. Agricult. Sci.* (1925). **15**(529–535).

[14] Willett, C.D., Adams, M.J., Johnson, S.A. and Seville, J.P.K. Capillary bridges between two spherical bodies. *Langmuir* (2000). **16**(24):9396–9405.

[15] Soulié, F., Cherblanc, F., El Youssoufi, M. and Saix, C. Influence of liquid bridges on the mechanical behaviour of polydisperse granular materials. *Int. J. Num. Anal. Meth. Geomech.* (2006). **30**(3):213–228.

[16] Richefeu, V., El Youssoufi, M.S., Peyroux, R. and Radjaï, F. A model of capillary cohesion for numerical simulations of 3d polydisperse granular media. *Int. J. Num. Anal. Meth. Geomech.* (2008). **32**(11):1365–1383.

[17] Lian, G., Thornton, C. and Adams, M. A theoretical study of the liquid bridge force between rigid spherical bodies. *J. Colloid Interface Sci.* (1993). **161**(1):138–147.

[18] Sveen, J.K. An introduction to matpiv v.1.6.1. Eprint no. 2, **ISSN** 0809-4403, Dept. of Mathematics, University of Oslo (2004). http://www.math.uio.no/~jks/matpiv.

[19] Westerweel, J., Dabiri, D. and Gharib, M. The effect of a discrete window offset on the accuracy of cross-correlation analysis of digital piv recordings. *Exp. Fluids* (1997). **23**:20–28.

[20] Cundall, P.A. and Strack, O.D.L. A discrete numerical model for granular assemblies. *Géotechnique* (1979). **29**(1):47–65.

[21] Bagi, K. A quasi-static numerical model for micro-level analysis of granular assemblies. *Mech. Mat.* (1993). **16**(1-2):101 – 110. Special Issue on Mechanics of Granular Materials.

[22] Kuhn, M.R. Structured deformation in granular materials. *Mech. Mat.* (1999). **31**(6):407 – 429.

[23] Silbert, L., Grest, G., Halsey, T., Levine, D. and Plimpton, S. Granular flow down an inclined plane: Bagnold scaling and rheology. *Phys. Rev. E* (2001). **64**:051302–1–14.